PHYSICAL REVIEW B **98**, 081404(R) (2018)

Rapid Communications

Cooling by heating in nonequilibrium nanosystems

R. Härtle,[1,2] C. Schinabeck,[3,2] M. Kulkarni,[4] D. Gelbwaser-Klimovsky,[5] M. Thoss,[3,2] and U. Peskin[6]
[1]*Institute of Theoretical Physics, University of Gottingen, 37077 Göttingen, Germany*
[2]*Institute of Physics, University of Freiburg, 79104 Freiburg, Germany*
[3]*Institute of Theoretical Physics and Interdisciplinary Center for Molecular Materials, University of Erlangen-Nuremberg, 91058 Erlangen, Germany*
[4]*International Centre for Theoretical Sciences, Tata Institute of Fundamental Research, Bangalore - 560089, India*
[5]*Department of Chemistry and Chemical Biology, Harvard University, Cambridge, Massachusetts 02138, USA*
[6]*Schulich Faculty of Chemistry, Technion-Israel Institute of Technology, Haifa 32000, Israel*

(Received 17 January 2018; revised manuscript received 28 May 2018; published 10 August 2018)

We demonstrate the possibility to reduce the heating of nanoelectronic systems in nonequilibrium situations by increasing the temperature of the environment. Such cooling by heating is possible for a variety of experimental conditions where the relevant transport-induced excitation processes become quenched and deexcitation processes are enhanced upon an increase of temperature. The phenomenon turns out to be robust with respect to all relevant parameters. It is especially pronounced for higher bias voltages and weak to moderate coupling. Our findings have implications for open quantum systems in general, where electron transport is coupled to mechanical (phononic) or photonic degrees of freedom. In particular, molecular junctions with rigid tunneling pathways or quantum dot circuit QED systems meet the required conditions.

DOI: 10.1103/PhysRevB.98.081404

Nanoelectronic systems exhibit a plethora of fundamentally interesting physical properties and, at the same time, are considered as promising architectures for technological applications, ranging from transistor [1,2] to quantum information devices [3,4]. Experimental realizations include single-molecule junctions [5–13], atomic wires [14–17], carbon nanotubes [18–24], and semiconductor based quantum dot systems [25–35]. A limiting factor is current-induced heating associated with the excitation of mechanical or electromagnetic degrees of freedom. Such heating limits the control, coherence, or even the mechanical stability of these devices. It is therefore expedient to identify and understand the intrinsic cooling mechanisms of nanoelectronic systems.

Nonequilibrium steady states offer the possibility for unprecedented control or cooling strategies. One possibility is to use the bias voltage which is applied to the device. In many situations, a nonzero voltage leads to additional heating processes and higher levels of excitation. However, in the presence of co-tunneling assisted sequential tunneling [36–38], higher-lying electronic states [39,40], antiresonances [41], suitably defined spectral properties of the leads [42,43], donor-acceptor structures [42,44–47], or electron-electron interactions [48], an increase in voltage can lead to lower excitation levels of the mechanical or photonic degrees of freedom. Another possibility is to use spin-polarized currents [49–51] and superconducting building blocks [52–59].

In this Rapid Communication, we use a different external variable, namely the temperature of the environment, and demonstrate how an increase leads to lower excitation levels of the nanoelectronic system and stabilizes the device. To be specific, we consider models of single-molecule junctions in the following. The principle, however, applies to any few-level systems where electron transport is coupled to mechanical or, e.g., in the case of cavity QED systems [23,24,32,33,35], photonic degrees of freedom. It is emphasized that our scheme for cooling by heating does not involve heat or temperature gradients such as in domestic [60] or quantum absorption refrigerators [61–66] or optomechanical devices [67]. Rather, a uniform heating of the environment reduces the excitation level that originates from inelastic transport processes.

The phenomenon of thermal stabilization predicted here is most strongly pronounced in the regime of weak to moderate molecule-lead and electronic-vibrational/photonic coupling and high enough (but still practically relevant) voltages, where transport-induced heating mechanisms [cf. Fig. 1(a)] are quenched for higher temperatures and, at the same time, cooling mechanisms are either less affected [cf. Fig. 1(b)] or become enhanced [cf. Fig. 1(c)]. An important characteristic of this regime is that weaker coupling to vibrational or photonic degrees of freedom results in higher excitation levels [48,68–73]. In the limit of vanishing couplings and temperatures, this leads to an indefinite increase of the excitation level for harmonic modes [71,73] that is a vibrational instability.[1]

We consider transport through a molecule (M) that is coupled to a left (L) and a right electrode (R). We describe this transport setup by the Hamiltonian $H = H_{\mathrm{M}} + H_{\mathrm{ME}} + H_{\mathrm{E}}$ where (using units where $\hbar = 1$ and $k_{\mathrm{B}} = 1$)

$$H_{\mathrm{M}} = \sum_{m\in\mathrm{M}} \epsilon_m d_m^\dagger d_m + \sum_{m<n\in\mathrm{M}} U_{mn} d_m^\dagger d_m d_n^\dagger d_n + H_{\mathrm{Vib}} + \sum_{m\in\mathrm{M}} \lambda_m (a + a^\dagger) d_m^\dagger d_m, \quad (1)$$

---

[1] Note that the term vibrational instability is also used in a slightly different context where internal heating processes emerge from a donor-acceptor structure of the molecule [46,47].

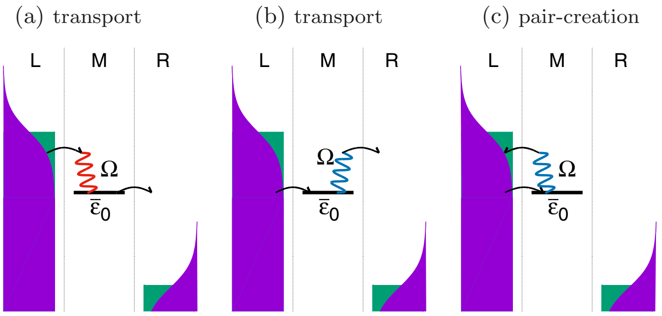

FIG. 1. Sketch of representative inelastic processes in a biased molecular junction, where electrons tunnel in two, sequential resonant tunneling processes onto and off the molecule (M). The green and purple areas represent occupied states in the left (L) and right lead (R) for lower and higher temperatures, respectively. Panel (a) and (b) depict transport processes, where the vibrational mode is excited and deexcited upon tunneling of an electron from L to M and from M to R, respectively. At low temperatures, process (a) requires higher bias voltages, $\Phi \gtrsim 2(\bar{\epsilon}_1 + \Omega)$, than process (b), $\Phi \gtrsim 2\bar{\epsilon}_1$. At these voltages, an increase of temperature reduces the initial state population of both processes. Panel (c) depicts a pair-creation process, where the electron returns to the original electrode. For $\Phi \gtrsim 2(\bar{\epsilon}_1 + \Omega)$ and low temperatures, this deexcitation process is Pauli blocked since its final state population is almost 1. It can be reactivated by an increase of temperature which reduces the final state population.

$$H_{\mathrm{Vib}} = \Omega a^\dagger a + \sum_\xi V_\xi (a + a^\dagger)^\xi, \tag{2}$$

$$H_{\mathrm{E}} = \sum_{k\in \mathrm{L,R}} \epsilon_k c_k^\dagger c_k + \sum_\alpha \omega_\alpha b_\alpha^\dagger b_\alpha, \tag{3}$$

$$\begin{aligned} H_{\mathrm{ME}} = &\sum_{m\in \mathrm{M}, k\in \mathrm{L,R}} (V_{mk} c_k^\dagger d_m + V_{mk}^* d_m^\dagger c_k) \\ &+ \sum_\alpha W_\alpha (a + a^\dagger)(b_\alpha + b_\alpha^\dagger). \end{aligned} \tag{4}$$

It includes a discrete set of electronic eigenstates with energies ϵ_m and density-density interactions U_{mn} between electrons in states m and n. The states of the molecule are coupled to a continuum of electronic states with energies ϵ_k and coupling matrix elements V_{mk} in the left (L) and the right (R) electrode. The corresponding tunneling efficiency or hybridization function is $\Gamma_{K,mn}(\epsilon) = 2\pi \sum_{k\in K} V_{mk}^* V_{nk} \delta(\epsilon - \epsilon_k)$ ($K \in \{\mathrm{L,R}\}$). Throughout this work, we use the wide-band approximation $\Gamma_{K,mn}(\epsilon) \approx \Gamma_{K,mn}$ and consider a symmetric drop of the applied bias voltage, i.e., the chemical potentials in the left and right lead are given by $\mu_{\mathrm{L/R}} = \pm\Phi/2$. We model vibrational effects by the vibrational Hamiltonian H_{Vib}, which, for $V_\xi = 0$, is harmonic with frequency Ω and, for nonzero V_ξ, includes generic anharmonic effects, most importantly a nonequidistant energy spectrum. The mode may be representative of the dominant reaction coordinate of the molecule. It is coupled to the electronic states of the molecule by coupling strengths λ_m and a bath of harmonic oscillators α with coupling strengths W_α in order to account for intramolecular vibrational energy redistribution [74–77] or energy losses to a bosonic junction's environment [78,79]. Note that we use the same temperature T to describe the bath and the electrodes, that is we do not consider any external temperature gradients, where, however, generalizations are straightforward and the phenomenon of thermal stabilization is not restricted to this choice.

We solve the above transport problem using the well established Born-Markov (BM) [39,48,68,80–84] and the recently developed hierarchical quantum master equation (HQME) approach [85]. Explicit formulas and detailed derivations for HQME and BM can be found in Refs. [85,86] and [48,71], respectively. The central quantity of both approaches is the reduced density matrix σ of the molecule which includes the electronic levels and the vibrational mode. We determine it as the stationary solution of its equation of motion,

$$0 \overset{!}{=} \frac{\partial \sigma(t)}{\partial t} = -i[H_{\mathrm{M}}, \sigma(t)] - \sigma^{(1)}(t), \tag{5}$$

where the first term of the rhs describes the internal dynamics of the molecule and the second term $\sigma^{(1)}(t)$ the influence of the environment. Using HQME, we determine $\sigma^{(1)}(t)$ by solving its equation of motion, which leads to second- and, consequently, higher-tier operators $\sigma^{(n)}(t)$ with $n > 1$. Truncation of this hierarchy corresponds to a truncated hybridization expansion. HQME thus allows us to systematically assess the importance of higher-order effects. The basic effect, however, is already included in BM, where the first-tier operator

$$\sigma^{(1)}(t) = \int_0^\infty d\tau\, \mathrm{tr}_{\mathrm{E}}\{[H_{\mathrm{ME}}, [H_{\mathrm{ME}}(\tau), \sigma(t)\sigma_{\mathrm{E}}]]\} \tag{6}$$

is expressed in terms of the reduced density matrix $\sigma(t)$, the density matrix of the environment σ_{E}, and the coupling operator $H_{\mathrm{ME}}(\tau) = \mathrm{e}^{-i(H_{\mathrm{M}}+H_{\mathrm{E}})\tau} H_{\mathrm{ME}} \mathrm{e}^{i(H_{\mathrm{M}}+H_{\mathrm{E}})\tau}$. Thus, BM corresponds to a first-tier truncation of HQME, including the Markov approximation $\sigma(t-\tau) \approx \mathrm{e}^{iH_{\mathrm{M}}\tau}\sigma(t)\mathrm{e}^{-iH_{\mathrm{M}}\tau}$ which enters the above integral kernel. In addition, we disregard off-diagonal elements of the density matrix and renormalization effects. A discussion on the role of vibrational off-diagonal elements can be found, for example, in Ref. [48]. The role of renormalization effects in the presence of electron-electron interactions has been outlined in Refs. [87–89], including a pronounced resonance in the conductance-voltage characteristics [90–92]. These effects, however, are not important for our discussion, which we show explicitly by a comparison to HQME where both off-diagonal elements and renormalization effects are included.

We introduce the phenomenon of thermal stabilization for a minimal model first. It includes a single electronic state with the polaron-shifted energy $\bar{\epsilon}_1 \equiv \epsilon_1 - \lambda_1^2/\Omega = 3\Omega$ that is weakly coupled to an undamped ($W_\alpha = 0$) harmonic mode with $\lambda_1 = \Omega/10$ and the leads with $\Gamma_{\mathrm{L/R},11} = \Omega/1000 \equiv \Gamma_{\mathrm{L/R}}$. We measure the stability of the junction by the average vibrational energy $\langle H_{\mathrm{Vib}}\rangle$. It is the result of thermal excitations, transport-induced excitation processes [Figs. 1(a)] and deexcitation processes which are associated either with transport [Fig. 1(b)] or pair-creation processes [Fig. 1(c)]. High values indicate a less stable junction, low ones a more stable junction. Hereafter, we associate changes in $\langle H_{\mathrm{Vib}}\rangle$ with *heating* or *cooling*. This practical terminology is useful [36–59], even though the nonequilibrium vibrational distribution is, in general, not thermal ($\langle H_{\mathrm{Vib}}\rangle$ corresponds to an effective vibrational temperature only in the weak coupling limits of the minimal model [43]).

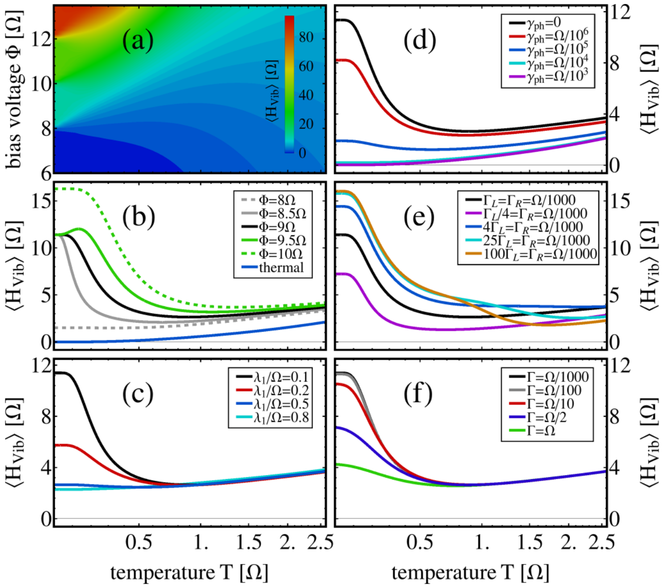

FIG. 2. Average vibrational energy $\langle H_{\text{Vib}}\rangle$ for our model of a molecular junction as a function of both temperature and applied bias voltage Φ [panel (a)], as a function of temperature for fixed voltages [panel (b)], different electronic-vibrational coupling strengths λ [panel (c)], mode-bath couplings [panel (d)], molecule-lead coupling ratios $\Gamma_{\text{L}}/\Gamma_{\text{R}}$ [panel (e)], and strengths Γ [panel (f)]. For the results shown in panels (c)–(f), we used $\Phi = 9\Omega$. If not stated otherwise, the other parameters are $\overline{\epsilon}_1 = 3\Omega$, $\lambda_1 = \Omega/10$, $\Gamma_{\text{L}} = \Gamma_{\text{R}} = \Omega/1000$, and $\gamma_{\text{ph}} = 2\pi \sum_\alpha |W_\alpha|^2 \delta(\Omega - \omega_\alpha)$. The results shown in panels (a)–(e) and (f) have been obtained using BM and HQME, respectively.

The average vibrational energy $\langle H_{\text{Vib}}\rangle$ of our minimal model is shown in Fig. 2(a) as a function of both bias voltage Φ and temperature T. At very low temperatures, $T \to 0$, we observe a steplike increase with bias voltage. The steps at $\Phi = 2(\overline{\epsilon}_1 + \Omega) = 8\Omega, 10\Omega, 12\Omega$... correspond to the opening of transport-induced heating processes [see Fig. 1(a)] and the closing of cooling processes via pair creation [see Fig. 1(c)], which are associated with single, two, three... phonon transitions, respectively. Increasing the temperature, the steps are smeared out and the vibrational energy decreases due to suppression (enhancement) of heating (cooling) processes as explained below.

We study this temperature effect more closely in Fig. 2(b) which shows the vibrational energy as a function of temperature for different fixed values of the applied bias voltage Φ. For low voltages $\Phi \lesssim 2(\overline{\epsilon}_1 + \Omega)$ (dashed gray line), the vibrational energy increases monotonically with temperature, starting from low transport-induced values which evolve towards values that are given by a thermal distribution [cf. the blue line which depicts the Bose function $1/(\exp(\Omega/T) - 1))$]. The vibrational energy is relatively low in this regime because transport-induced heating is outbalanced by both transport-induced cooling [Fig. 1(b)] and pair-creation processes [Fig. 1(c)] [48]. Additional heating processes [Fig. 1(a)] become active at higher bias voltages $\Phi \gtrsim 2(\overline{\epsilon}_1 + \Omega)$, while, in parallel, pair-creation processes with a single phonon transition become blocked [e.g., the one depicted in Fig. 1(c)]. Thus, the transport-induced vibrational energy increases significantly at these voltages (cf. solid and dashed green lines). This leads to a qualitatively different temperature dependence, in particular a negative slope in an intermediate temperature regime, which becomes more pronounced for higher bias voltages. This is the regime where thermal stabilization occurs, that is a decrease of the vibrational energy as the temperature of the environment is increased. The mechanism can be rationalized by the effect of thermal broadening which quenches preferentially the additional heating processes [compare Fig. 1(a) to Fig. 1(b)] and allows pair-creation processes [Fig. 1(c)] to cool the junction again before thermal fluctuations override any transport-induced effects. For very low temperatures, $T \ll \Omega/2$, these broadening effects are too inefficient, as reflected by the plateau which appears before the average vibrational energy decreases. The small peak in the green line indicates the onset of transport-induced excitation processes [Fig. 1(a)] and the suppression of pair creation processes [Fig. 1(c)] with two vibrational quanta which, for $\Phi = 9.5\Omega$, occurs before pair-creation processes with a single vibrational quantum become re-activated. Notice that when the leads temperature exceeds the vibration quantum, $T \gtrsim \Omega$, the negative slope changes into a positive one. This is the regime where the energy content in the vibration is set by the leads temperature. Also notice that the vibration does not cool below the leads temperature.

As will be shown below, the phenomenon of thermal stabilization is robust. Nevertheless, the extent of the regime where thermal stabilization occurs depends on the specific junction parameters which we now study one by one. To this end, we point out that the phenomenon occurs in the same regime of bias voltages, $\Phi \gtrsim 2(\overline{\epsilon}_1 + \Omega)$, where the model exhibits a vibrational instability as $\lambda, T, \Gamma_{\text{L/R}} \to 0$, that is an indefinite increase of vibrational energy as the electronic-vibrational coupling constant is decreased [68–73]. Consequently, the transport-induced vibrational energy is higher and the stabilization effect is more pronounced for weaker electronic-vibrational coupling, as can be seen in Fig. 2(c), where we show the temperature dependence of the vibrational energy for different electronic-vibrational coupling strengths. While the vibrational energy of the mode is indeed lower for stronger coupling strengths, a negative slope can still be seen for intermediate coupling strengths, i.e., $\lambda/\Omega \lesssim 0.5$.

Another parameter of the model is the energy of the electronic level with respect to the Fermi level of the junction. Thermal stabilization, however, turns out to be rather insensitive to this parameter, unless additional pair-creation processes, e.g., with respect to the electrode with the lower chemical potential, come into play [93]. The same is true, when additional electronic states are included, even in the presence of electron-electron interactions [93].

At this point, we increase the complexity of our model by coupling the vibrational mode to a heat bath. Figure 2(d) shows the average vibrational energy $\langle H_{\text{Vib}}\rangle$ of the extended model as a function of temperature for different mode-bath coupling strengths. The overall effect of the bath is to reduce the vibrational energy and, consequently, to narrow the range of temperatures where an increase in temperature leads to a reduction of the vibrational energy. Nevertheless, thermal stabilization is observed also in the presence of coupling to a heat bath. We also point out that, for $\gamma_{\text{ph}} = \Omega/10^5$ (blue line), the level of vibrational energy at $T < 0.5\Omega$ is similar to the minimum one for $\gamma_{\text{ph}} = \Omega/10^6$ and $\gamma_{\text{ph}} = 0$ (red and black lines). Thus, we estimate the cooling power of thermal stabilization to be $\sim\Omega^2/10^5$ for this set of parameters.

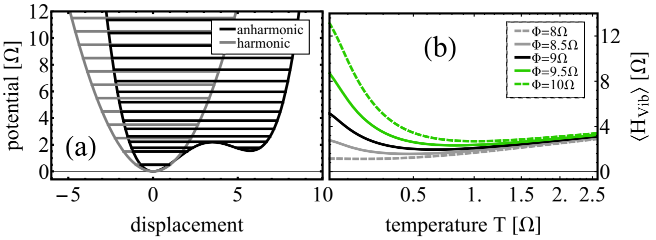

FIG. 3. Panel (a): Potential of the vibrational motion for $V_2 = 0.136\Omega$, $V_3 = 0.084\Omega$, and $V_4 = 0.005\Omega$. Panel (b): Average vibrational energy $\langle H_{\mathrm{Vib}}\rangle$ as a function of temperature for $\epsilon_1 = 3\Omega$ and the anharmonic potential shown in panel (a). We used BM to obtain these results.

So far, we considered symmetric coupling to the leads. Thus, the rate of transport and pair-creation processes differ only by thermal factors. Asymmetric molecule-lead coupling, $\Gamma_{\mathrm{L}} \neq \Gamma_{\mathrm{R}}$, affects the balance between transport and pair-creation processes, leading, for example, to vibrational rectification [48] or mode-selective vibrational excitation [94,95]. Figure 2(e) shows the average vibrational energy for our minimal model of a molecular junction as a function of temperature for different asymmetry scenarios. If the lead with the higher chemical potential is more strongly coupled to the molecule, cooling via pair-creation processes is more effective. The corresponding reduction of vibrational energy has a similar effect as coupling of the mode to a heat bath. In the opposite case, where the lead with the higher chemical potential is less strongly coupled to the molecule, cooling via pair-creation processes is less effective. Consequently, the average vibrational energy at low temperatures increases and the stabilization regime extends over a broader range of temperatures. In this regime, the quenching of heating processes is the dominant mechanism for thermal stabilization, in particular for $\Gamma_{\mathrm{L}} \lesssim \Gamma_{\mathrm{R}}/100$.

Next, we discuss the effect of higher-order processes and broadening due to the hybridization of the molecule with the leads. To this end, we employ the HQME approach and symmetric coupling to the leads ($\Gamma_{\mathrm{L}} = \Gamma_{\mathrm{R}} = \Gamma$). Figure 2(f) shows converged data for the average vibrational energy as a function of temperature for different molecule-lead coupling strengths. In the antiadiabatic regime $\Gamma \ll \Omega$ (black line), we recover the BM results. Increasing the coupling strength, the average vibrational energy at low temperatures decreases. We attribute this behavior to broadening effects due to the hybridization of the molecule with the leads which have a similar effect as an increased thermal broadening. Accordingly, the stabilization effect is most pronounced in the antiadiabatic regime, where BM theory applies.

Last but not least, we demonstrate that the phenomenon of thermal stabilization is not restricted to harmonic vibrations. To this end, we relax the harmonic approximation and consider an anharmonic potential [see black line in Fig. 3(a)]. The corresponding average vibrational energy is depicted in Fig. 3(b). Despite differences to the harmonic case, the anharmonic system still exhibits a pronounced regime where thermal stabilization occurs. Qualitative changes occur at low temperatures, because transport-induced and pair-creation processes can now take place at a variety of energies, redistributing the onset voltages for excitation and deexcitation processes. Thus, e.g., the plateau at low temperatures ($T \ll \Omega$) is less pronounced.

We conclude that molecular junctions exhibit a broad range of parameters where they can be stabilized by increasing the temperature of the environment. As we showed, the stabilization effect is robust and occurs in the weak- to intermediate-coupling regime at voltages where resonant pair-creation processes with a single or more vibrational quanta [cf. Fig. 1(c)] are suppressed. This suppression is typical for low temperatures, i.e., $T \lesssim \Omega$. An increase in temperature leads to unbalanced transport-induced cooling and heating processes which favors the former and to a gradual reactivation of cooling by pair creation, resulting in a reduction of the vibrational energy. The phenomenon is more pronounced at even higher bias voltages and in the antiadiabatic regime $\Gamma \lesssim \Omega$ and occurs for weak to intermediate electronic-vibrational coupling. We also observe it in more complex models with multiple electronic and vibrational degrees of freedom as well as for anharmonic vibrations. Our findings obtained for the specific example of molecular junctions apply similarly to other nanoelectronic systems, in particular circuit QED systems where the tunneling electrons interact with photonic instead of vibrational degrees of freedom.

This work was supported by the Israel Science Foundation (ISF), the German Research Foundation (DFG), and the German-Israeli Foundation for Scientific Research and Development (GIF).

---

[1] P. G. Piva, G. A. DiLabio, J. L. Pitters, J. Zikovsky, M. Rezeq, S. Dogel, W. A. Hofer, and R. A. Wolkow, Nature (London) **435**, 658 (2005).
[2] H. Song, Y. Kim, Y. H. Jang, H. Jeong, M. A. Reed, and T. Lee, Nature (London) **462**, 1039 (2009).
[3] D. Loss and D. P. DiVincenzo, Phys. Rev. A **57**, 120 (1998).
[4] K. D. Petersson, L. W. McFaul, M. D. Schroer, M. Jung, J. M. Taylor, A. A. Houck, and J. R. Petta, Nature (London) **490**, 380 (2011).
[5] M. A. Reed, C. Zhou, C. J. Muller, T. P. Burgin, and J. M. Tour, Science **278**, 252 (1997).
[6] J. Reichert, R. Ochs, D. Beckmann, H. B. Weber, M. Mayor, and H. v. Lohneysen, Phys. Rev. Lett. **88**, 176804 (2002).
[7] J. Park, A. N. Pasupathy, J. I. Goldsmith, C. Chang, Y. Yaish, J. R. Petta, M. Rinkoski, J. P. Sethna, H. D. Abruna, P. L. McEuen *et al.*, Nature (London) **417**, 722 (2002).
[8] M. A. Reed, Nat. Mater. **3**, 286 (2004).
[9] S. W. Wu, G. V. Nazin, X. Chen, X. H. Qiu, and W. Ho, Phys. Rev. Lett. **93**, 236802 (2004).
[10] G. Cuniberti, G. Fagas, and K. Richter, *Introducing Molecular Electronics* (Springer, Heidelberg, 2005).

[11] L. Venkataraman, J. E. Klare, C. Nuckolls, M. S. Hybertsen, and M. L. Steigerwald, Nature (London) **442**, 904 (2006).

[12] D. Secker, S. Wagner, S. Ballmann, R. Härtle, M. Thoss, and H. B. Weber, Phys. Rev. Lett. **106**, 136807 (2011).

[13] J. C. Cuevas and E. Scheer, *Molecular Electronics: An Introduction To Theory And Experiment* (World Scientific, Singapore, 2010).

[14] N. Agrait, C. Untiedt, G. Rubio-Bollinger, and S. Vieira, Chem. Phys. **281**, 231 (2002).

[15] N. Agrait, A. L. Yeyati, and J. M. van Ruitenbeek, Phys. Rep. **377**, 81 (2003).

[16] J. Schäfer, S. Meyer, C. Blumenstein, K. Roensch, R. Claessen, S. Mietke, M. Klinke, T. Podlich, R. Matzdorf, A. A. Stekolnikov *et al.*, New J. Phys. **11**, 125011 (2009).

[17] C. Blumenstein, J. Schäfer, S. Mietke, S. Meyer, A. Dollinger, M. Lochner, X. Y. Cui, L. Patthey, R. Matzdorf, and R. Claessen, Nat. Phys. **7**, 776 (2011).

[18] B. J. LeRoy, S. G. Lemay, J. Kong, and C. Dekker, Nature (London) **432**, 371 (2004).

[19] S. J. Tans, M. H. Devoret, H. Dai, A. Thess, R. Smalley, L. J. Geerligs, and C. Dekker, Nature (London) **386**, 474 (1997).

[20] S. Sapmaz, P. Jarillo-Herrero, Y. M. Blanter, and H. S. J. van der Zant, New J. Phys. **7**, 243 (2005).

[21] S. Sapmaz, P. Jarillo-Herrero, Y. M. Blanter, C. Dekker, and H. S. J. van der Zant, Phys. Rev. Lett. **96**, 026801 (2006).

[22] R. Leturcq, C. Stampfer, K. Inderbitzin, L. Durrer, C. Hierold, E. Mariani, M. G. Schultz, F. von Oppen, and K. Ensslin, Nat. Phys. **5**, 327 (2009).

[23] M. R. Delbecq, V. Schmitt, F. D. Parmentier, N. Roch, J. J. Viennot, G. Fève, B. Huard, C. Mora, A. Cottet, and T. Kontos, Phys. Rev. Lett. **107**, 256804 (2011).

[24] M. R. Delbecq, L. E. Bruhat, J. J. Viennot, S. Datta, A. Cottet, and T. Kontos, Nat. Commun. **4**, 1400 (2013).

[25] M. A. Reed, J. N. Randall, R. J. Aggarwal, R. J. Matyi, T. M. Moore, and A. E. Wetsel, Phys. Rev. Lett. **60**, 535 (1988).

[26] B. J. van Wees, H. van Houten, C. W. J. Beenakker, J. G. Williamson, L. P. Kouwenhoven, D. van der Marel, and C. T. Foxon, Phys. Rev. Lett. **60**, 848 (1988).

[27] A. W. Holleitner, C. R. Decker, H. Qin, K. Eberl, and R. H. Blick, Phys. Rev. Lett. **87**, 256802 (2001).

[28] W. G. van der Wiel, S. De Franceschi, J. M. Elzerman, T. Fujisawa, S. Tarucha, and L. P. Kouwenhoven, Rev. Mod. Phys. **75**, 1 (2002).

[29] T. Ihn, M. Sigrist, K. Ensslin, W. Wegscheider, and M. Reinwald, New J. Phys. **9**, 111 (2007).

[30] G. Kießlich, E. Schöll, T. Brandes, F. Hohls, and R. J. Haug, Phys. Rev. Lett. **99**, 206602 (2007).

[31] D. Tutuc, B. Popescu, D. Schuh, W. Wegscheider, and R. J. Haug, Phys. Rev. B **83**, 241308 (2011).

[32] J. J. Viennot, M. R. Delbecq, M. C. Dartiailh, A. Cottet, and T. Kontos, Phys. Rev. B **89**, 165404 (2014).

[33] Y. Y. Liu, K. D. Petersson, J. Stehlik, J. M. Taylor, and J. R. Petta, Phys. Rev. Lett. **113**, 036801 (2014).

[34] A. Beckel, A. Kurzmann, M. Geller, A. Ludwig, A. D. Wieck, J. König, and A. Lorke, Eur. Phys. Lett. **106**, 47002 (2014).

[35] Y. Liu, J. Stehlik, C. Eichler, M. J. Gullans, J. M. Taylor, and J. R. Petta, Science **347**, 285 (2015).

[36] M. C. Lüffe, J. Koch, and F. von Oppen, Phys. Rev. B **77**, 125306 (2008).

[37] A. K. Hüttel, B. Witkamp, M. Leijnse, M. R. Wegewijs, and H. S. J. van der Zant, Phys. Rev. Lett. **102**, 225501 (2009).

[38] F. Santandrea, L. Y. Gorelik, R. I. Shekhter, and M. Jonson, Phys. Rev. Lett. **106**, 186803 (2011).

[39] R. Härtle, C. Benesch, and M. Thoss, Phys. Rev. Lett. **102**, 146801 (2009).

[40] G. Romano, A. Gagliardi, A. Pecchia, and A. Di Carlo, Phys. Rev. B **81**, 115438 (2010).

[41] E. J. McEniry, T. N. Todorov, and D. Dundas, J. Phys.: Condens. Matter **21**, 195304 (2009).

[42] M. Galperin, K. Saito, A. V. Balatsky, and A. Nitzan, Phys. Rev. B **80**, 115427 (2009).

[43] D. Gelbwaser-Klimovsky, A. Aspuru-Guzik, M. Thoss, and U. Peskin, Nano Lett. **18**, 4727 (2018).

[44] S. Zippilli, G. Morigi, and A. Bachtold, Phys. Rev. Lett. **102**, 096804 (2009).

[45] Z. Li, S. Ouyang, C. Lam, and J. Q. You, Europhys. Lett. **95**, 40003 (2011).

[46] J. T. Lü, P. Hedegård, and M. Brandbyge, Phys. Rev. Lett. **107**, 046801 (2011).

[47] L. Simine and D. Segal, Phys. Chem. Chem. Phys. **14**, 13820 (2012).

[48] R. Härtle and M. Thoss, Phys. Rev. B **83**, 115414 (2011).

[49] J. Brüggemann, S. Weiss, P. Nalbach, and M. Thorwart, Phys. Rev. Lett. **113**, 076602 (2014).

[50] P. Stadler, W. Belzig, and G. Rastelli, Phys. Rev. Lett. **113**, 047201 (2014).

[51] P. Stadler, W. Belzig, and G. Rastelli, Phys. Rev. B **91**, 085432 (2015).

[52] I. Martin, A. Shnirman, L. Tian, and P. Zoller, Phys. Rev. B **69**, 125339 (2004).

[53] D. A. Rodrigues, J. Imbers, and A. D. Armour, Phys. Rev. Lett. **98**, 067204 (2007).

[54] K. R. Brown, J. Britton, R. J. Epstein, J. Chiaverini, D. Leibfried, and D. J. Wineland, Phys. Rev. Lett. **99**, 137205 (2007).

[55] F. Xue, Y. D. Wang, Y.-x. Liu, and F. Nori, Phys. Rev. B **76**, 205302 (2007).

[56] G. Sonne, M. E. Peña-Aza, L. Y. Gorelik, R. I. Shekhter, and M. Jonson, Phys. Rev. Lett. **104**, 226802 (2010).

[57] G. Sonne and L. Y. Gorelik, Phys. Rev. Lett. **106**, 167205 (2011).

[58] P. Stadler, W. Belzig, and G. Rastelli, Phys. Rev. Lett. **117**, 197202 (2016).

[59] P. Stadler, W. Belzig, and G. Rastelli, Phys. Rev. B **96**, 045429 (2017).

[60] M. Gordon and K. C. Ng, *Cool Thermodynamics* (Cambridge International Science Publishing, Cambridge, England, 2000).

[61] J. P. Palao, R. Kosloff, and J. M. Gordon, Phys. Rev. E **64**, 056130 (2001).

[62] N. Linden, S. Popescu, and P. Skrzypczyk, Phys. Rev. Lett. **105**, 130401 (2010).

[63] A. Levy and R. Kosloff, Phys. Rev. Lett. **108**, 070604 (2012).

[64] B. Cleuren, B. Rutten, and C. Van den Broeck, Phys. Rev. Lett. **108**, 120603 (2012).

[65] D. Gelbwaser-Klimovsky and G. Kurizki, Phys. Rev. E **90**, 022102 (2014).

[66] D. Gelbwaser-Klimovsky, W. Niedenzu, and G. Kurizki, Adv. At. Mol. Opt. Phys. **64**, 329 (2015).

[67] A. Mari and J. Eisert, Phys. Rev. Lett. **108**, 120602 (2012).

[68] A. Mitra, I. Aleiner, and A. J. Millis, Phys. Rev. B **69**, 245302 (2004).

[69] J. Koch, M. Semmelhack, F. von Oppen, and A. Nitzan, Phys. Rev. B **73**, 155306 (2006).

[70] R. Avriller, J. Phys.: Condens. Matter **23**, 105301 (2011).

[71] R. Härtle and M. Thoss, Phys. Rev. B **83**, 125419 (2011).

[72] D. Kast, L. Kecke, and J. Ankerhold, Beilstein J. Nanotechnol. **2**, 416 (2011).

[73] R. Härtle and M. Kulkarni, Phys. Rev. B **91**, 245429 (2015).

[74] S. Mukamel and R. E. Smalley, J. Chem. Phys. **73**, 4156 (1980).

[75] K. F. Freed and A. Nitzan, *Energy Storage and Redistribution in Molecules* (Plenum, New York, 1983).

[76] A. H. Zewail, *Femtochemistry – Ultrafast Dynamics of the Chemical Bond* (World Scientific, Singapore, 1994).

[77] D. J. Nesbitt and R. W. Field, J. Phys. Chem. **100**, 12735 (1996).

[78] N. J. Tao, Nat. Nano. **1**, 173 (2006).

[79] R. Jorn and T. Seidemann, J. Chem. Phys. **131**, 244114 (2009).

[80] V. May, Phys. Rev. B **66**, 245411 (2002).

[81] J. Lehmann, S. Kohler, V. May, and P. Hänggi, J. Chem. Phys. **121**, 2278 (2004).

[82] U. Harbola, M. Esposito, and S. Mukamel, Phys. Rev. B **74**, 235309 (2006).

[83] R. Volkovich, M. Caspary Toroker, and U. Peskin, J. Chem. Phys. **129**, 034501 (2008).

[84] I. A. Pshenichnyuk and M. Čížek, Phys. Rev. B **83**, 165446 (2011).

[85] C. Schinabeck, A. Erpenbeck, R. Härtle, and M. Thoss, Phys. Rev. B **94**, 201407 (2016).

[86] J. Jin, X. Zheng, and Y. Yan, J. Chem. Phys. **128**, 234703 (2008).

[87] J. König and J. Martinek, Phys. Rev. Lett. **90**, 166602 (2003).

[88] B. Wunsch, M. Braun, J. König, and D. Pfannkuche, Phys. Rev. B **72**, 205319 (2005).

[89] R. Härtle and A. J. Millis, Phys. Rev. B **90**, 245426 (2014).

[90] R. Härtle, G. Cohen, D. R. Reichman, and A. J. Millis, Phys. Rev. B **88**, 235426 (2013).

[91] M. Hell, B. Sothmann, M. Leijnse, M. R. Wegewijs, and J. König, Phys. Rev. B **91**, 195404 (2015).

[92] S. Wenderoth, J. Bätge, and R. Härtle, Phys. Rev. B **94**, 121303(R) (2016).

[93] See Supplemental Material at http://link.aps.org/supplemental/10.1103/PhysRevB.98.081404 for detailed results where we varied the position of the electronic level, added a second electronic level and even included electron-electron interactions.

[94] R. Härtle, R. Volkovich, M. Thoss, and U. Peskin, J. Chem. Phys. **133**, 081102 (2010).

[95] R. Volkovich, R. Härtle, M. Thoss, and U. Peskin, Phys. Chem. Chem. Phys. **13**, 14333 (2011).